Applied Mathematics & Information Sciences
An International Journal

http://dx.doi.org/10.12785/amis/080634

Haar Wavelet Approach for Numerical Solution of Two Parameters Singularly Perturbed Boundary Value Problems

Sapna Pandit[1,*] *and Manoj Kumar*

Department of Mathematics, Motilal Nehru National Institute of Technology Allahabad, 211004(U.P), India

Received: 4 Nov. 2013, Revised: 2 Feb. 2014, Accepted: 3 Feb. 2014
Published online: 1 Nov. 2014

Abstract: In this paper, we proposed an efficient numerical method based on uniform Haar wavelet for the numerical solutions of two parameter singularly perturbed boundary value problems. Such type of problems arise in various field of science and engineering, such as heat transfer problem with large Peclet numbers, Navier-Stokes flows with large Reynolds numbers, transport phenomena in chemistry and biology, chemical reactor theory, aerodynamics, reaction-diffusion process, quantum mechanics, optimal control theory etc. In present study more accurate solutions have been obtained by wavelet decomposition with multiresolution analysis. An extensive amount of error analysis has been carried out to obtain the convergence of the method. Four test problems are considered to check the efficiency and accuracy of the proposed method. The numerical results are found in good agreement with exact and existing solutions in literature.

Keywords: Haar wavelets, Singular perturbation, Convection diffusion, Reaction diffusion, Self-adjoint differential equation.

1 . Introduction

The present paper deals Haar wavelet method to find the numerical solutions of the two-parameter singularly perturbed boundary value problems

$$Ly \equiv -\epsilon a(x)y'' + \mu b(x)y' + c(x)y = f(x) \quad x \in (0,1) \tag{1}$$

subject to the boundary conditions

$$y(0) = \alpha, y(1) = \beta \tag{2}$$

with two small parameters, $0 < \epsilon \ll 1$ and $0 \ll \mu \ll 1$. The functions $a(x), b(x), c(x)$ and $f(x)$ are assumed to be sufficiently smooth real valued function and satisfied $a(x) \geq a^* \geq 0$, $b(x) \geq b^* > 0$ and $c(x) \geq c^* \geq 0$ for $x \in (0,1)$. Under these assumptions the problem (1) is characterized in three cases: For $\mu = 0$ problem (1) becomes reaction diffusion problem with boundary layer of width $o(\epsilon)$ at $x = 0$ and for $\mu = 1$ problem (1) is reduced in convection-diffusion problem with boundary layer of width $o(\sqrt{\epsilon})$ in the neighbourhood of $x = 0$ and $x = 1$. For $\mu b(x) = a^{'}(x)$ problem (1) is self adjoint problem.

It is well known that singularly perturbed problems often have very thin boundary layers and internal layers where the solution varies rapidly, whereas away from the layer, solution behaves regularly and varies slowly. So the numerical treatment of singularly perturbed problems faces major difficulties. A large number of research papers and books have been published describing various methods for solving singular perturbation problems [1–17].

Due to the variation in the width of the layer with respect to the small perturbation parameters several difficulties are experienced in solving the singular perturbation problems using standard numerical methods with uniform mesh. There are three principal approaches to solve numerically the model equation (1), namely, finite difference method, finite element method and spline approximation [5–9, 14].

In recent years, wavelet approach is becoming more popular in the field of numerical approximations. Different types of wavelets and approximating functions have been used for this purpose. Any function of $L^2(R)$ can be expressed by the dilation and translation of wavelet functions, so it had drawn a great deal of

* Corresponding author e-mail: sappu15maths@gmail.com

attention from scientists and engineers. Wavelets especially adopted to solve the equation with the singular solution and local severe gradients. Wavelets have many excellent properties such as exact representation of polynomials to a certain degree, flexibility to represent functions at different levels of resolution.

The Haar wavelets have gained popularity among researchers and scientists for their useful properties such as simple applicability, orthogonality and compact support. Compact support of the Haar wavelet basis allows straight inclusion of the different types of boundary conditions in the numerical algorithms. An essential shortcoming of Haar wavelets is that it is not continuous, that is derivatives do not exist at the point of discontinuity, therefore it is not possible to apply the Haar wavelets directly to solve differential equations. There are two possibilities of ending this stand still situation. First, piecewise constant Haar functions can be regularized with the spline interpolation that generates the complexity in the solution. Another possibility is to expand all functions into Haar series in place of Haar function itself. The detail discussion of Haar wavelets and its applications can be seen in [10–13].

In this paper we have applied the technique of Haar wavelet method to approximate highest derivative appearing in the differential equation by Haar series and the other derivatives are obtained through integration of Haar series. The integration of Haar wavelet is preferred because the differentiation of Haar wavelet always results impulse functions. Through integration we can expand differential equation into Haar matrix H with Haar coefficient matrix P of $2M \times 2M$ order on collocation points. The main idea of this technique is to convert a differential equation into algebraic one. In order to approximate the solution of differential equation we collocate the algebraic equations at collocation points. The benefits of Haar wavelet transform are sparse matrix of representation; possibility of implementation of fast algorithms, the method is more accurate with less computations than other existing methods. In this article the error analysis is carried out that shows! high order convergence can be achieved on increasing the value of M to obtain the desired approximation.

The paper is organized as: Section 2 gives a brief description of the Haar wavelet. The derivation of the Haar wavelet transform scheme for various cases of two parameter singularly perturbed problem has been described in Section 3. In Section 4 we present the convergence analysis of Haar wavelet method. In Section 5 we consider four numerical problems for comparison with existing methods. The conclusion is given in Section 6.

2 . The Haar Wavelets and its Theoretical Aspects

Haar function had been used since 1910 and it was introduced by Hungarian mathematician Alfred Haar [11]. Haar function is an odd rectangular pulse pair that is the simplest and oldest orthonormal wavelet with compact support. There are different definitions of Haar function and its various generalization had been discussed in the literature. Alfred Haar shown that certain square wave function could be translated and scaled to create a basis set that span L^2. After one year, it was seen that the system of Haar functions is a particular wavelet system. If we choose scaling function to have compact support over $0 \leq x \leq 1$, that is the Haar wavelet family for $x \in [0, 1]$ and defined as

$$h_i(x) = \begin{cases} 1, & x \in [\xi_1, \xi_2) \\ -1, & x \in [\xi_2, \xi_3) \\ 0, & otherwise \end{cases}$$

where

$$\xi_1 = \frac{k}{m}, \quad \xi_2 = \frac{k + 0.5}{m}, \quad \xi_3 = \frac{k + 1}{m} \tag{3}$$

integer $m = 2^j$, $j = 0, 1, 2, ..., J$ indicates the level of wavelet and integer $k = 0, 1, 2, ...m - 1$ is the translation parameter and J is Maximal level of resolution. The index i in equation (3) is calculated from the formula $i = m + k + 1$. In the case of minimal values $m = 1$, $k = 0$ we have $i = 2$. The maximum value of i is given by $i = 2M = 2^{J+1}$. For $i = 1$, the function $h_1(x)$ is the scaling function for the family of the Haar wavelets and defined by

$$h_1(x) = \begin{cases} 1, & x \in [0, 1) \\ 0, & otherwise \end{cases} \tag{4}$$

In the Haar wavelet method the following integrals are used

$$P_{1,i}(x) = \begin{cases} x - \xi_1, & x \in [\xi_1, \xi_2) \\ \xi_3 - x, & x \in [\xi_2, \xi_3) \\ 0, & otherwise \end{cases} \tag{5}$$

$$P_{2,i}(x) = \begin{cases} \frac{(x-\xi_1)^2}{2}, & x \in [\xi_1, \xi_2) \\ \frac{1}{4m^2} - \frac{(\xi_3 - x)^2}{2}, & x \in [\xi_2, \xi_3) \\ \frac{1}{4m^2}, & x \in [\xi_3, 1) \\ 0, & otherwise \end{cases} \tag{6}$$

In general

$$P_{v+1,i}(x) = \int_0^x P_{v,i}(x')dx' \tag{7}$$

where $v = 1, 2, 3, ...$

$$C_{1,i}(x) = \int_0^1 P_{1,i}(x)dx \tag{8}$$

Any function $g(x)$ which is square integrable in the interval $(0,1)$ can be expressed in the following form of Haar wavelet

$$g(x) = \sum_{i=0}^{\infty} a_i h_i(x) \tag{9}$$

The above series terminates at finite terms if $g(x)$ is piecewise constant or can be approximated as piecewise constant in each subinterval. The best way to understand the wavelets is through a multi-resolution analysis. If a function $g \in L^2(R)$, a multiresolution analysis (MRA) of $L^2(R)$ produces a sequence of subspaces $U_j, U_{j+1}, ...$ such that the projection of g onto these spaces provides finer and finer approximations of the function g as $j \to 0$.

2.1 Multiresolution Analysis

In this section, we shall study the construction of the wavelet and the properties of multiresolution analysis. A multiresolution analysis of $L^2(R)$ is defined as a sequence of closed subspaces $U_j \in L^2(R)$,$j \in Z$ with the following properties

(a) $0... \subset U_{-1} \subset U_0 \subset U_1 \subset ...L^2$
(b) the space U_j satisfy $\cup_{j\in Z} U_j$ is dense in $L^2(R)$ and $\cap_{j\in Z} U_j = \{0\}$
(c) If $g(x) \in U_0(x)$, $g(2^j(x)) \in U_j(x)$ i.e. the spaces are scaled version of the central space U_0
(d) If $g(x) \in U_0(x)$, $g(2^j(x) - k) \in U_j(x)$ i.e. all the U_j are invariant under translation.
(e) There exists $\phi \in U_0$ such that $\phi(x-k), k \in Z$ is a Riesz basis in U_0 .

The space U_j is used to approximate general functions by defining appropriate projection of these functions onto these spaces. Since the union of all U_0 is dense in $L^2(R)$, so it guarantees that any function in $L^2(R)$ can be approximated arbitrarily close by such projections. As an example the space U_0 can be defined as $U_j = W_{j-1} \oplus U_{j-1} = W_{j-1} \oplus W_{j-2} \oplus U_{j-2} = ... = \oplus_{j=0}^{j-1} W_j \oplus U_0$ then the scaling function $h_1(x)$ generates an MRA for the sequence of spaces $U_j, j \in Z$ by translation and dilation in property (c) and (d). For each j the space W_j serves as the orthogonal complement of U_j in U_{j+1} . The space W_j includes all the functions in U_{j+1} that are orthogonal to all those spaces in U_j under some chosen inner product. The set of functions which form basis for the space W_j are called wavelets [12, 13]. In Haar wavelet the approximate solution can be expressed in term of scaling function basis $h_i(x)$at scale J as.

$$g(x) = \sum_{i=0}^{2^{(J+1)}-1} a_i h_i(x)$$

3 . Haar Wavelet Method for solving differential equations

To construct a simple and accurate Haar wavelet method for problem (1) we approximate highest order derivative $y^{''}(x)$ using Haar wavelet series as follows

$$y^{''}(x) = \sum_{i=0}^{2M-1} a_i h_i(x) \tag{10}$$

On integrating equation (10) we get $y^{'}(x), y(x)$ and finally $y(x)$ can be expanded in form of Haar wavelet series and its integrals [26–28].

$$y^{'}(x) = \sum_{i=0}^{2M-1} a_i P_{1,i}(x) + y^{'}(0) \tag{11}$$

$$y(x) = \sum_{i=0}^{2M-1} a_i (P_{2,i}(x) + y^{'}(0))x + y(0) \tag{12}$$

where $P_{1,i}, P_{2,i}$ are defined in equation (5) and (6).
The presence of two integration constants allow us the addition of two extra equations which can be done by using information on the governing equation and boundary conditions at both ends of the line. Discretization using collocation points $x_z = \frac{z-0.5}{2M}$ $z = 0,1,2,3,...,2M-1$ of equations (10)-(12) can be reduced into the following matrix form

$$y^{''} = \begin{bmatrix} h_0(x_0) & ... & h_{2M-1}(x_0) & 0 & 0 \\ & ... & ... & ... & ... \\ h_0(x_{2M-1}) & ... & h_{2M-1}(x_{2M-1}) & 0 & 0 \end{bmatrix} \begin{bmatrix} a \\ b \end{bmatrix} \tag{13}$$

$$y^{'} = \begin{bmatrix} P_{1,0}(x_0) & ... & P_{1,2M-1}(x_0) & 1 & 0 \\ & ... & ... & ... & ... \\ P_{1,0}(x_{2M-1}) & ... & P_{1,2M-1}(x_{2M-1}) & 1 & 0 \end{bmatrix} \begin{bmatrix} a \\ b \end{bmatrix} \tag{14}$$

$$y = \begin{bmatrix} P_{2,0}(x_0) & ... & P_{2,2M-1}(x_0) & x_0 & 1 \\ & ... & ... & ... & ... \\ P_{2,0}(x_{2M-1}) & ... & P_{2,2M-1}(x_{2M-1}) & x_{2M-1} & 1 \end{bmatrix} \begin{bmatrix} a \\ b \end{bmatrix} \tag{15}$$

The boundary condition can be transformed into

$$\begin{bmatrix} y(0) \\ y(1) \end{bmatrix} = \begin{bmatrix} P_{2,0}(0) & ... & P_{2,2M-1}(0) & 0 & 1 \\ P_{2,0}(1) & ... & P_{2,2M-1}(1) & 1 & 1 \end{bmatrix} \begin{bmatrix} a \\ b \end{bmatrix} \tag{16}$$

where $a = [a_0, a_1, ..., a_{2M-1}]^T$ and $b = [y^{'}(0), y(0)]^T$.
To calculate $y^{'}(0)$ we integrate equation (11) from 0 to 1 then we have

$$y^{'}(0) = y(1) - y(0) + \sum_{i=0}^{2M-1} a_i C_{1,i} \tag{17}$$

Now substitute the values of $y^{''}(x)$, $y^{'}(x)$ and $y(x)$ in equation (1) and we get non homogeneous system of algebraic equations which contains $2M$ equations and $2M$ unknowns. On solving this system using back slash command in Matlab we obtain the Haar coefficients. The approximate solution can be determined using Haar coefficients $a_i, i = 0,1,2,...2M-1$ in equation (12).

4 . Error Analysis

In this section we employ the error analysis for the proposed scheme. In order to check the convergence of the proposed scheme we consider the asymptotic expansion of equation (12) as given below

$$Y(x) = \alpha + (\beta - \alpha)x + \sum_{i=0}^{\infty} a_i(P_{2,i}(x) - xC_{1,i}) \quad (18)$$

The error estimation as J^{th} resolution level is

$$|Y(x) - y(x)| = |e_J(x)| = |\sum_{i=2M}^{\infty} a_i(P_{2,i}(x) - xC_{1,i}| \quad (19)$$

$$||e_J(x)||^2 = |\int_{-\infty}^{\infty} \sum_{i=2^{J+1}}^{\infty} \sum_{n=2^{J+1}}^{\infty} a_i a_n \left(P_{2,i}(x) - xC_{1,i}\right)\left(P_{2,n}(x) - xC_{1,n}\right)dx| \quad (20)$$

$$||e_J(x)||^2 = |\sum_{i=2^{J+1}}^{\infty} \sum_{n=2^{J+1}}^{\infty} \int_{-\infty}^{\infty} a_i a_n \left(P_{2,i}(x) - xC_{1,i}\right)\left(P_{2,n}(x) - xC_{1,n}\right)dx| \quad (21)$$

$$\leq \sum_{i=2^{J+1}}^{\infty} \sum_{n=2^{J+1}}^{\infty} a_i a_n K_{i,n} dx \quad (22)$$

where $K_{i,n} \neq (0) \in R,\ \forall n = 2^{J+1}, 2^{J+1}+1, \quad \cdots$

and $K_i = \sup_{n=2^{J+1}}^{\infty} K_{i,n}$ (23)

But $a_n = \int_0^1 2^{\frac{j}{2}} y(x)h(2^j x - k), k = 0, 1, 2, ..., 2^j - 1$ and $j = 0, 1, ...J$

$$h_i(2^j x - k) = \begin{cases} 1 & k2^{-j} \leq x < (k + \frac{1}{2})2^{-j} \\ -1 & (k + \frac{1}{2})2^{-j} \leq x < (k + 1)2^{-j} \\ 0 & otherwise \end{cases} \quad (24)$$

Therefore

$$a_n = 2^{\frac{j}{2}}\left(\int_{k2^{-j}}^{(k+\frac{1}{2})2^{-j}} y(x)dx - \int_{(k+\frac{1}{2})2^{-j}}^{(k+1)2^{-j}} y(x)dx\right)$$

$$= 2^{\frac{j}{2}}((k + \frac{1}{2})2^{-j} - (k)2^{-j})y(\eta_2) - 2^{\frac{j}{2}}((k + 1)2^{-j} - (k + \frac{1}{2})2^{-j})y(\eta_1) \quad (25)$$

where

$$\eta_1 \in ((k)2^{-j} - (k + \frac{1}{2})2^{-j}),$$

$$\eta_2 \in ((k)2^{-j} - (k + \frac{1}{2})2^{-j})$$

consequently we have

$$a_n = 2^{\frac{j}{2}-1}(y(\eta_2) - y(\eta_1))$$

Applying mean value theorem

$$a_n = 2^{-\frac{j}{2}-1}(\eta_2 - \eta_1)y'(\eta),$$

where $\quad \eta \in (K2^{-j}, (K + 1)2^{-j})$

$$a_n \leq 2^{-\frac{j}{2}-1}2^{-j}D = 2^{\frac{-3j-2}{2}}D, \quad \text{since } y'(\eta) \leq D$$

$$||e_J(x)||^2 \leq \sum_{i=2^{J+1}}^{\infty} a_i K_i \sum_{n=2^{J+1}}^{\infty} a_n \quad (26)$$

$$\leq \sum_{i=2^{J+1}}^{\infty} a_i K_i \sum_{n=2^{J+1}}^{\infty} 2^{\frac{-3j-2}{2}} D$$

$$\leq \sum_{i=2^{J+1}}^{\infty} D a_i K_i \sum_{n=2(J+1)}^{\infty} \sum_{n=2^{\frac{j}{2}}}^{2^{\frac{j}{2}+1}-1} 2^{\frac{-3j-2}{2}}$$

$$\leq \sum_{i=2^{J+1}}^{\infty} D a_i K_i \sum_{n=2(J+1)}^{\infty} 2^{\frac{-3j-2}{2}} \; 2^{\frac{j}{2}}$$

$$\leq \sum_{i=2^{J+1}}^{\infty} D a_i K_i \sum_{n=2(J+1)}^{\infty} 2^{-j-1}$$

$$\leq \sum_{i=2^{J+1}}^{\infty} D a_i K_i \frac{2^{-2(J+1)-1}}{1 - \frac{1}{4}} \quad (27)$$

Similarly $a_i \leq D2^{\frac{-3j}{2}-1}$ and $K = \sup_{i=2^{j+1}}^{\infty} (K_i)$

Therefore

$$||e_J(x)||^2 \leq D^2 K \sum_{j=2(J+1)}^{\infty} 2^{\frac{-3j}{2}-1}2^{\frac{j}{2}}\left(\frac{2^{-2(J+1)-1}}{1 - \frac{1}{4}}\right)$$

$$\leq D^2 K \sum_{j=2(J+1)}^{\infty} 2^{-j-1}\left(\frac{2^{-2(J+1)-1}}{1 - \frac{1}{4}}\right)$$

$$\leq D^2 K\left(\frac{2^{-2(J+1)-1}}{1 - \frac{1}{4}}\right)\left(\frac{2^{-2(J+1)-1}}{1 - \frac{1}{4}}\right)$$

$$||e_J(x)||^2 \leq D^2 K\left(\frac{2^{-2(J+1)-1}}{1 - \frac{1}{4}}\right)\left(\frac{2^{-2(J+1)-1}}{1 - \frac{1}{4}}\right) \quad (28)$$

$$||e_J(x)||^2 \leq D^2 K\left(\frac{2^{-2(J+1)-1}}{1 - \frac{1}{4}}\right)^2$$

$$||e_J(x)||^2 \leq 2D\sqrt{K}\left(\frac{2^{-2(J+1)}}{3}\right)^2 \quad (29)$$

From equation (29) we can clearly conclude that $||e_J(x)|| \rightarrow 0$ when $J \rightarrow 0$ i.e. error is inversely proportional to the resolution of the Haar wavelet J. Thus the proposed composite scheme is convergent.

5 . Numerical Experiment and Discussion

To demonstrate the applicability of the method, we consider four singular perturbed problems which have been widely discussed in the literature and exact solutions are available for comparison. First three problems are reaction diffusion and self-adjoint problems for $\mu = 0$, $\mu b(x) = a(x)^{'}$ in equation (1) and last problem is convection diffusion problem for $\mu = 1$.

Problem 1:

$$\epsilon y'' + y = -(cos^2(\pi x) + 2\epsilon\pi^2 cos(2\pi x)) \quad x \in (0,1) \tag{30}$$

with boundary conditions

$$y(0) = 0, y(1) = 1 \tag{31}$$

The exact solution of the problem is given by

$$y(x) = \frac{e^{(-(1-x)/\sqrt{\epsilon})} + e^{(-(x)/\sqrt{\epsilon})}}{1 + e^{(-(1)/\sqrt{\epsilon})}} \tag{32}$$

The numerical results of the problem are shown in Tables 1-3 and in Figures $1, 2$. Table 1 shows the maximum absolute error at different values of M for small values of ϵ. Tables $2, 3$ provide a comparison of maximum absolute error with the existing methods [6, 20, 25] and it is concluded that the present method gives better results than [6, 20, 25]. Figure 1 compares the exact and numerical solutions while Figure 2 depicts the physical behaviour of the problem for different values of ϵ.

Problem 2:

$$\epsilon y'' + y = -40[x(x^2 - 1) - 2\epsilon] \quad x \in (0,1) \tag{33}$$

with boundary conditions

$$y(0) = 0, y(1) = 0 \tag{34}$$

The exact solution of the problem is given by

$$y(x) = 40x(1-x) \tag{35}$$

Tables $4, 5$ and Figures $3, 4$ report the numerical results of the problem 2. Table 4 shows the maximum absolute error for different values of M and ϵ while Table 5 presents a comparison of maximum absolute error with the existing methods [6, 17–19]and it is concluded that proposed method gives better results. Figure 3 compares the exact and numerical solutions while Figure 4 depicts the physical behavior of the problem for different values of ϵ.

Problem 3:

$$-\epsilon y'' + (1 + x(1-x))y = 1 + x(1-x) + (2\sqrt{\epsilon} - x^2(1-x)e^{(-(1-x)/\sqrt{\epsilon})}) \tag{36}$$

$$y(0) = 0, y(1) = 1 \tag{37}$$

The exact solution of the problem is given by

$$y(x) = 1 + (x-1)e^{(-x/\sqrt{\epsilon})} - x\, e^{-(1-x)\sqrt{(\epsilon)}} \tag{38}$$

Table 6 shows the maximum absolute error of the Problem 3 for different values of ϵ and M. Tables 7 compare the maximum absolute error with different methods [20, 21] and it is concluded that our method gives better results. Figures $5 - 6$ show a comparison of numerical and exact solutions while Figure 7 depicts numerical behavior of the problem for different values of ϵ. From Table 7 and Figure 6 following are the observations:-

- When M is fixed and ϵ decreases then maximum absolute error decreases slowly and increases rapidly near to $\epsilon = 10^{-7}$.
- When ϵ is fixed and M is increasing then maximum absolute error decreases.
- When ϵ and M both are fixed then maximum absolute error is large as $x \to 0$ and $x \to 1$.

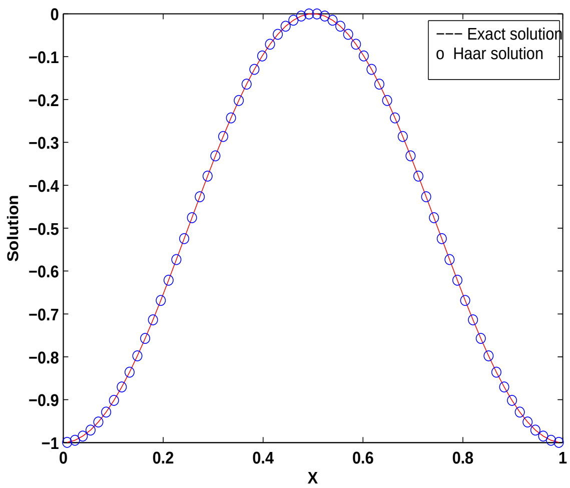

Fig. 1: Physical behaviour of exact and numerical solutions of problem 1 for $\epsilon = 2^{-25}$ and $M = 32$.

Problem 4:

$$\epsilon y'' + \mu y' + y = cos(\pi x) \qquad x \in (0,1) \tag{39}$$

with boundary conditions

$$y(0) = 0, y(1) = 1 \tag{40}$$

The exact solution of the probelm is given by

$$y(x) = a_1 cos(\pi x) + b_1 sin(\pi x) + Ae^{(\lambda_1 x)} + Be^{(-\lambda_2(1-x))} \tag{41}$$

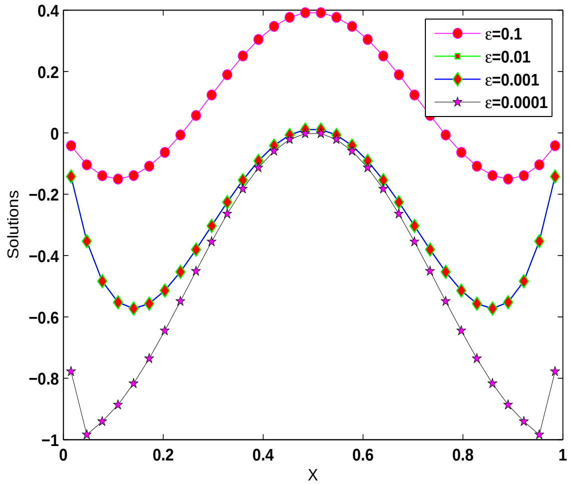

Fig. 2: Physical behavior of numerical solutions of problem 1 for different values of ϵ and $M = 16$.

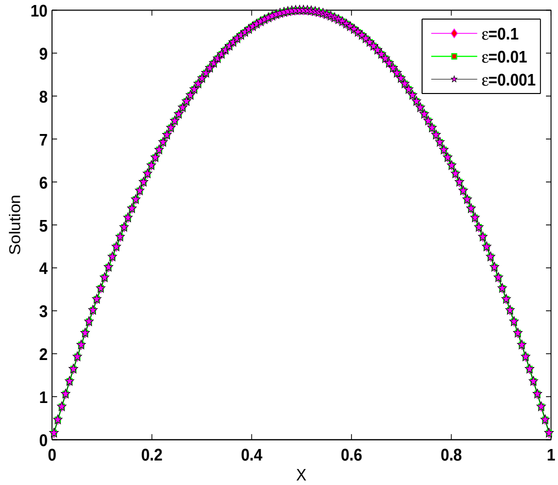

Fig. 4: Physical behavior of numerical solution of problem 2 for different values of ϵ and $M = 64$.

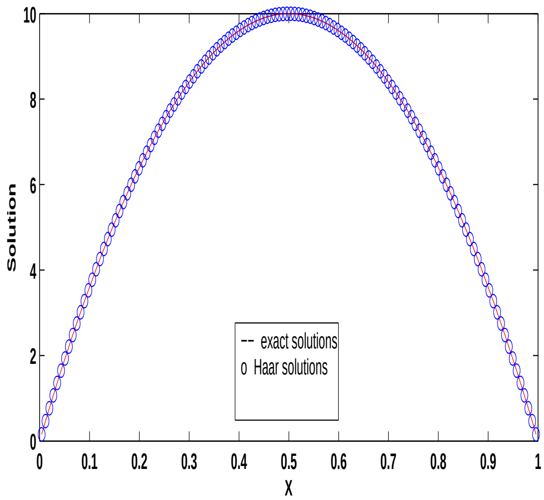

Fig. 3: Physical behaviour of exact and numerical solutions of problem 2 for $\epsilon = 10^{-3}$ and $M = 64$.

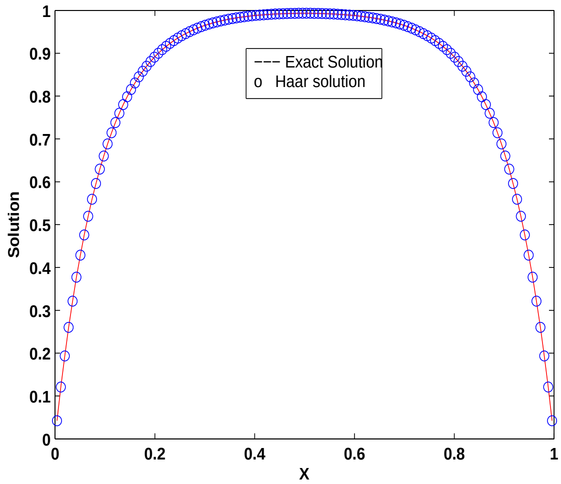

Fig. 5: Physical behavior of exact and numerical solutions of problem 3 for $\epsilon = 10^{-2}$ and $M = 64$.

where

$$a_1 = \frac{\epsilon\pi^2 + 1}{\mu^2\pi^2 + (\epsilon\pi^2 + 1)^2}, \quad b_1 = \frac{p\pi}{\mu^2\pi^2 + (\epsilon\pi^2 + 1)^2} \tag{42}$$

$$A = \frac{-a(1 + e^{(-\lambda_2)})}{1 - e^{(\lambda_1 - \lambda_2)}}, \quad A = \frac{a(1 + e^{(\lambda_1)})}{1 - e^{(\lambda_1 - \lambda_2)}} \tag{43}$$

and λ_1, λ_2 are the roots of the characteristic equation $-\epsilon\lambda^2 + \mu\lambda + 1 = 0$. The numerical results of the problem are shown in Table 8 and Figures $8 - 10$. Table 8 presents a comparison of maximum absolute error with the existing methods [22, 24] and it is concluded that our method gives better results. Figure 8 compares the exact and numerical solutions while Figures $9 - 10$ depict same physical behavior of the problem for different values of ϵ and fixed value of $\mu = 10^6$ as shown in [23]. For this problem it is observed that when ϵ decreases $\mu = 10^{-6}$, $M = 128$, the error increases as shown in Table 10. From Figure $8 - 10$ it is concluded that the width of boundary

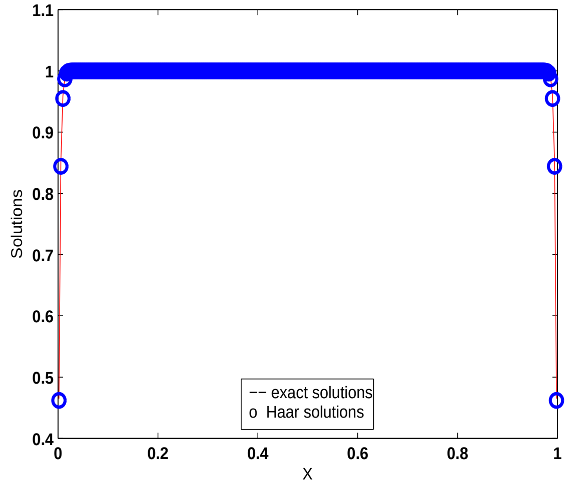

Fig. 6: : Physical behavior of exact and numerical solutions of problem 3 for $\epsilon = (10)^{-5}$ and $M = 256$.

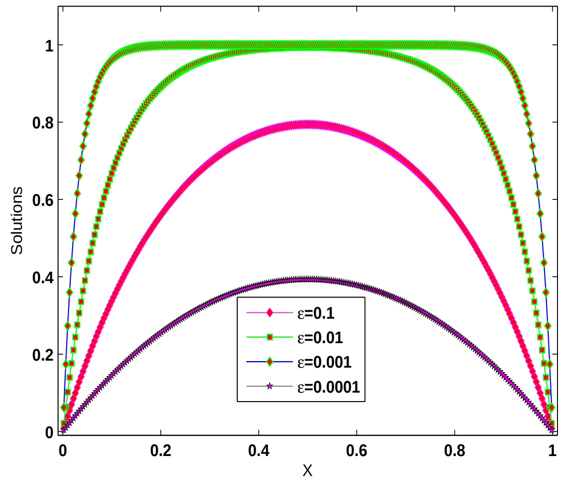

Fig. 7: Physical behavior of numerical solution of problem 3 for different values of ϵ and $M = 128$.

layer decreases and wave shape becomes more and more stiff at $x = 0$ and $x = 1$.

6 . Conclusion

In the present study, numerical solutions of two parameters singularly perturbed boundary-value problems; reaction diffusion, self adjoint problem and convection diffusion problem are discussed using Haar

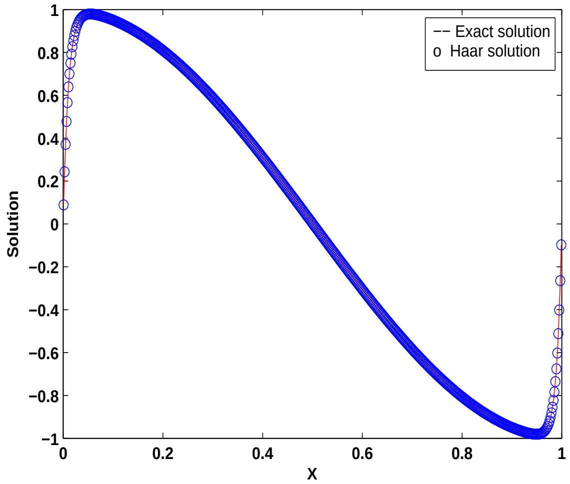

Fig. 8: Physical behavior of exact and numerical solutions of problem 4 for $\epsilon = (10)^{-4}$, $\mu = (10)^{-3}$, $M = 256$.

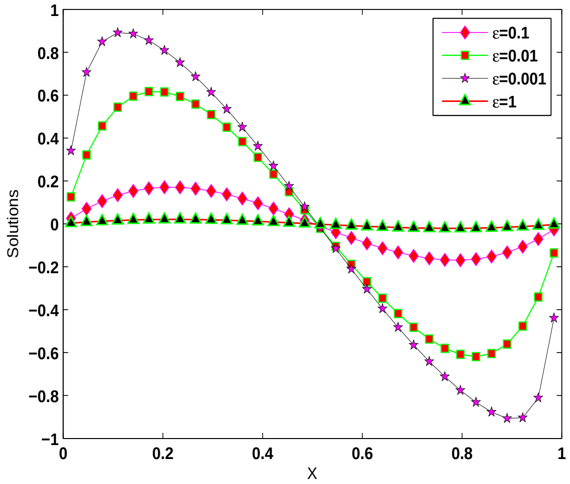

Fig. 9: Physical behavior of numerical solution of problem 4 for different values of ϵ, $\mu = (10)^{-2}$, $M = 16$.

wavelets method. The proposed method is computationally efficient and the algorithm can be easily implemented on computer. The Haar solutions are very good in agreement with exact solutions and solutions available in literature [6, 17, 22, 24, 25]. The comparison with analytical solution shows that Haar wavelet gives better results with less computational cost: it is due to the sparsity of the transform matrix and small number of wavelet coefficients. It is worth mentioning that Haar

Table 1: Maximum absolute error of problem 1 for different values of M and small value of ϵ

$\epsilon = 2^{-K}$	M=16	M=32	M=64	M=128	M=256	M=512	M=1024
K= 6	5.07E-4	1.27E-4	3.18E-5	7.94E-6	1.98E-6	4.96E-7	1.24E-7
K= 10	6.10E-3	1.80E-3	4.68E-4	1.19E-4	2.98E-5	7.46E-6	1.87E-6
K= 20	3.20E-3	1.23E-2	2.93E-2	1.94E-2	1.27E-2	6.10E-3	1.80E-3
K= 25	1.01E-4	4.04E-4	1.60E-3	6.40E-3	2.13E-2	2.92E-2	1.44E-2
K= 30	3.16E-6	1.26E-5	5.05E-5	2.02E-4	8.08E-4	3.20E-3	1.23E-2
K= 35	9.88E-8	3.95E-7	1.58E-6	6.32E-6	2.53E-5	1.01E-4	4.04E-4
K= 40	3.09E-9	1.23E-8	4.93E-8	1.97E-7	7.90E-7	3.16E-6	1.26E-5
K= 45	9.64E-11	3.86E-10	1.54E-9	6.17E-9	2.47E-8	9.87E-8	3.97E-7
K= 50	3.01E-12	1.20E-11	4.82E-11	1.93E-10	7.72E10	3.09E-9	1.23E-8

Table 2: Comparision of maximum absolute error of problem 1 for different values of M and $\epsilon = 2^{-K}$

$\epsilon = 2^{-K}$	Kadalbajoo et.al. [6]	Present method	$\epsilon = (2^{-K})^2$	Bawa et.al. [25]	Present method
K= 10	5.022E-2	1.80E-3	K= 10	5.022E-2	1.23E-2
K= 20	3.125E-2	1.23E-3	K= 20	3.125E-2	1.23E-8
K= 25	3.125E-2	4.04E-4	K= 25	3.125E-2	1.20E-11

Table 3: Comparison of maximum absolute error of problem 1 for different values of M and $\epsilon = 10^{-K}$.

$\epsilon = 10^{-K}$	$M = 2^4$		$M = 2^6$		$M = 2^8$	
	Kumar [20]	Present method	Kumar [20]	Present method	Kumar [20]	present method
K=3	0.55E-1	5.97E-3	0.10E-1	4.57E-4	0.27E-2	2.91E-5
K=4	0.28E-1	1.44E-2	0.44E-1	4.06E-3	0.69E-2	2.89E-4
K=5	0.31E-2	2.49E-3	0.42E-1	1.39E-3	0.34E-1	2.60E-4
K=7	0.31E-4	3.39E-4	0.56E-3	5.37E-3	0.90E-2	3.02E-2

Table 4: Maximum absolute error of problem 2 for different values of M and $\epsilon = 10^{-K}$

$\epsilon = 10^{-K}$	M=16	M=32	M=64	M=128	M=256	M=512	M=1024
K=3	3.55E-15	5.32E-15	6.22E-15	1.06E-14	1.06E-14	1.24E-14	8.89E-15
K=4	1.24E-14	5.15E-14	1.24E-14	2.13E-14	1.06E-14	2.31E-14	3.82E-14
K=5	2.11E-11	2.66E-14	6.57E-14	1.08E-13	7.81E-14	5.50E-14	6.21E-14
K=6	4.08E-14	5.50E-14	2.36E-13	1.69E-13	3.35E-13	4.24E-13	2.30E-13
K=7	2.30E-14	9.06E-14	2.14E-13	1.01E-13	8.01E-13	9.17E-13	2.15E-12
K=8	2.30E-14	2.49E-14	1.88E-13	3.29E-13	1.18E-12	1.34E-12	1.69E-12

Table 5: Comparison of maximum absolute error of problem 2 for different values of M and $\epsilon = 10^{-K}$

$\epsilon = 10^{-K}$	Miller [19]	Niijima [18]	Niijima [17]	Kadalbajoo [6]	Present Method
K= 3	0.64E-02	0.65E-02	0.65E-04	1.776E-15	1.77E-015
K= 6	0.77E-03	0.31E-02	0.33E-04	1.776E-15	5.32E-015
K= 9	0.00E+00	0.13E-03	0.11E-04	1.789E-15	8.88E-015

Table 6: Maximum absolute error of problem 3 for different values of M and $\epsilon = 2^{-K}$

$\epsilon = 2^{-K}$	M=16	M=32	M=64	M=128	M=256	M=512	M=1024
K=6	6.14E-4	1.56E-4	3.91E-5	9.80E-6	2.45E-6	6.12E-7	1.53E-7
K=10	6.40E-3	1.90E-3	5.01E-4	1.28E-4	3.21E-5	8.03E-6	2.00E-6
K=20	3.20E-3	1.22E-2	2.92E-2	1.94E-2	1.27E-2	6.10E-3	1.80E-3
K=25	9.96E-5	4.01E-4	1.60E-3	6.40E-3	2.13E-2	2.92E-2	1.44E-2
K=30	3.11E-6	1.25E-5	5.03E-5	2.02E-4	8.07E-4	3.20E-3	1.23E-2
K=35	9.73E-8	3.92E-7	1.57E-6	6.30E-6	2.52E-5	1.01E-4	4.04E-4
K=40	3.04E-9	1.22E-8	4.92E-8	1.97E-7	7.89E-7	3.15E-6	1.26E-5

Table 7: Comparison of maximum absolute error of problem 3 for different values of ϵ and M.

$\epsilon = 10^{-K}$	$M = 2^4$			$M = 2^7$		
	Kumar [20]	Lubuma [21]	Present method	Kumar [20]	Lubuma [21]	Present method
K=1	0.72E-2	0.94E-3	2.03E-4	0.11E-2	0.24E-3	3.18E-6
K=2	0.24E-1	0.57E-2	8.93E-4	0.42E-2	0.15E-2	1.44E-5
K=3	0.77E-1	0.28E-1	6.32E-3	0.29E-2	0.11E-1	1.24E-4
K=5	0.46E-2	0.53E-2	2.46E-3	0.82E-1	0.13E-2	8.14E-3
K=7	0.46E-4	0.53E-2	3.33E-4	0.35E-2	0.13E-2	1.88E-3
K=7	0.46E-8	0.53E-2	3.34E-8	0.35E-6	0.13E-2	2.16E-6

Table 8: Comparisons of maximum absolute error with other existing methods of problem 4 for different values of ϵ, μ.

μ	$\epsilon = 10^{-2}, M = 128$			$\epsilon = 10^{-4}, M = 128$		
	Kadalbajoo et.al [22]	Zahra [24]	Present Method	Kadalbajoo et.al. [22]	Zahra [24]	Present Method
10^{-3}	8.3832-5	4.1924-5	4.2303 E-5	9.4446-3	4.7598-3	5.1964E-3
10^{-4}	8.2686-5	4.1296-5	4.1318 E-5	9.0436-3	4.2856-3	4.1710E-3
10^{-5}	8.2572-5	4.1232-5	4.1220E-5	9.0036-3	4.2295-3	4.0754E-3
10^{-6}	8.2561-5	4.1226-5	4.1210E-5	8.9996-3	4.2238-3	4.0659E-3
10^{-7}	8.2559-5	4.1225-5	4.1209E-5	8.9992-3	4.2232-3	4.0650E-3

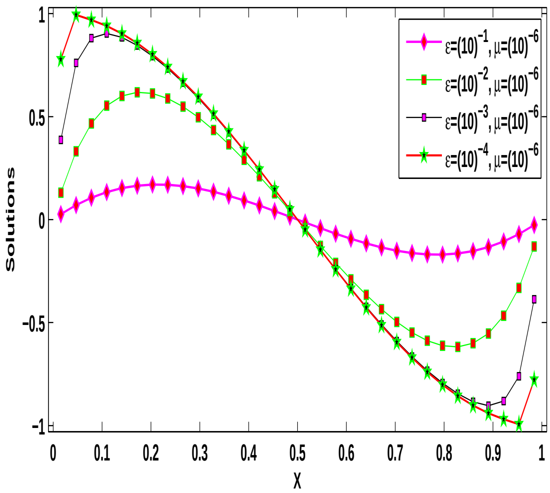

Fig. 10: Physical behavior of numerical solution of problem 4 for different values of ϵ, μ, $M = 32$.

wavelet provides excellent results for small and large values of M.

Acknowledgement

The authors would like to express their sincere thanks to the editor in chief, editor and reviewers for their valuable suggestions to revise the manuscript.

References

[1] K. Surla, Z. Uzelac, L. Teofanov, The discrete minimum principle for quadratic spline discretization of a singularly perturbed problem, Mathematics and Computers in Simulation, **79**, 2490-2505 (2009) .

[2] W. Eckhaus, Asymptotic analysis of singular perturbations, North Holland, New York, (1979).

[3] R. E. O'Malley, Introduction to singular perturbations, Academic Press, New York, (1974).

[4] E. Riordan, M. L. Pickett, Singularly perturbed problems modeling reaction-convection-diffusion process, Computational Methods in Applied Mathematics, **3**, 424-442 (2003).

[5] V. Vukoslavecevic, K. Surla, Finite element method for solving self-adjoint singularly perturbed boundary value problems, Math. Montisnigri, **8**, 89-96 (1996).

[6] M. K. Kadalbajoo, V. K. Aggarwal, Fitted mesh B-spline collocation method for solving self-adjoint singularly perturbed boundary value problems, Applied Mathematics and Computation, **161**, 973-987 (2005).

[7] S. C. Rao, M. Kumar, Exponential B-spline collocation method for self-adjoint singularly perturbed boundary value problems, Applied Numerical Mathematics, **58**, 1572-1581 (2008).

[8] M. K. Kadalbajoo, D. Kumar, Variable mesh finite difference method for self-adjoint singularly perturbed two point boundary value problems, Journal of Computational Mathematics, **28**, 711-724 (2010).

[9] A. Ashyralyev, H. O. Fattorini On uniform difference schemes for second order singular perturbation Problems in Banach spaces, SIAM Journal of Mathematical Analysis, **23**, 29-54 (1992).

[10] U. Lepik, Numerical solution of differential equations using Haar wavelets, Mathematics and Computers in Simulation, **68**, 127-143 (2005).

[11] A. Haar, Zur Theorie der orthogonalen Funktionensysteme, (Erste Mitteilung), Mathematische Annalem, **69**, 331-37 (1910).

[12] J. C. Goswami, Chan, Fundamentals of Wavelets. Theory, Algorithms, and Applications, John Wiley and Sons, New York, (1999).

[13] S. Mallat, A Wavelet tour of signal processing, 2nd ed., Academic Press, New York, (1999).

[14] H. K. Mishra, M. Kumar, P. Singh, Initial value technique for self-adjoint singular perturbation boundary value problems, Computational Mathematics and Modeling, **20**, (2009).

[15] S. Islam, I. Aziz, B. Sarler,The numerical solution of second-order boundary-value problems by collocation method with the Haar wavelets, Mathematical and Computer Modelling, **52**, 1577-1590 (2010).

[16] H. Hashish, S. H. Behiry, N. A. El-Shamy, Numerical integration using wavelets, Applied Mathematics and Computation, Applied Mathematics and Computation, **211**, 480-487 (2009).

[17] K. Niijima, On a three-point difference scheme for a singular perturbation problem without a first derivative term II, Mem. Numer. Math, **7**, 11-27 (1980).

[18] K. Niijima, On a three-point difference scheme for a singular perturbation problem without a first derivative term I, Mem. Numer. Math, **7**, 1-10 (1980).

[19] J. J. H. Miller, On the convergence, uniformly in ϵ, of difference schemes for a two-point boundary singular perturbation problem, Numerical Analysis of Singular Perturbation Problems, Academic Press, New York, 467-474 (1979).

[20] V. Kumar, M. Mehra, Wavelet optimized finite difference method using interpolating wavelets for self-adjoint singularly perturbed problems, Journal of Computational and Applied Mathematics, **230**, 803-812 (2009).

[21] J. M.S. Lubuma, K. C. Patidar, Uniformly convergent non-standard finite difference methods for self-adjoint singular perturbation problems, Journal of Computational and Applied Mathematics, **191**, 228-238 (2006).

[22] M. K. Kadalbajoo, A. S. Yadaw, B-spline collocation method for a two-parameter singularly perturbed convection-diffusion boundary value problem, Applied Mathematics and Computation, **201**, 504-513 (2008).

[23] B. Lin, K. Li, Z. Cheng, B-spline solution of a singularly perturbed boundary value problem arising in biology, Chaos, Solitons and Fractals, **42**, 2934-2948 (2009).

[24] W. K. Zahra, Ashraf M. El Mhlawy, Numerical solution of two-parameter singularly perturbed boundary value problems via exponential spline, Journal of King Saud University Science, 1-8 (2013).

[25] R. K. Bawa, S. Natesan, A computational method for self adjoint singular perturbation problem using quintic spline, Computers and Mathematics with Applications, **50**, 1371-1382 (2005).

[26] M. Kumar, S. Pandit, A composite numerical scheme for the numerical simulation of coupled Burgers' equation, Computer Physics Communications, **185**, 809-817 (2014).

[27] R. Jiwari, A Haar wavelet quasilinearization approach for numerical simulation of Burgers' equation, Computer Physics Communications, **183**, 2413-2423 (2012).

[28] Z. Shi, Y. Cao, Q. Chen, Solving 2D and 3D Poisson equations and biharmonic equations by the Haar wavelet method, Applied Mathematical Modelling, doi:10.1016/j.apm.2011.11.078 (2012).

Sapna Pandit was born in Kurukshetra, India, in 1987. She received the M.Sc degree from Gurukul Kangri University, Haridwar, India. She is currently working toward the Ph.D. degree at Motilal Nehru National Institute of Technology (MNNIT), Allahabad, India. Her research interests include wavelet analysis/Numerical analysis/Partial Differential Equations.

Manoj Kumar was born in Aligarh, India, in 1975. He received his Ph.D. degree from Aligarh Muslim University, Aligarh, India, in 2000. He joined Motilal Nehru National Institute of Technology (MNNIT), Allahabad, as Assistant Professor in 2005 and Associate Professor in 2010. His current research interests are Numerical Analysis/Mathematical Modeling/Partial Differential Equations/Computational Fluid Dynamics. Currently he has more than sixty research paper in reputed journals.